

# HYBRID POSITION AND VIBRATION CONTROL OF NONLINEAR CRANE SYSTEM

N. M. Tahir<sup>1, 2\*</sup>, A. G. Ibrahim<sup>1</sup>, H. Liman<sup>1</sup>

<sup>1</sup>Faculty of Engineering, Abu bakar Tafawa Balewa University, PMB 0248, Bauchi,  
Nigeria

<sup>2</sup>Faculty of Electrical Engineering, Universiti Teknologi Malaysia, 81310 UTM, Johor,

## ABSTRACT

*This paper presents comparative assessments of input shaping techniques using two different approaches, for sway reduction of cranes system. First, the shaper was designed at maximum load hoisting length while the second was designed at average load hoisting length. These were accomplished using curve fitting toolbox in MATLAB. In both case; Zero Vibration (ZV), Zero Vibration Derivative (ZVD) and Zero Vibration Derivative Derivatives (ZVDD) were designed. Average hoisting length (AHL) shapers performed better than the Maximum hoisting length (MHL) shapers. Proportional integral derivative (PID) was incorporated for position control. After successful implementation, Simulation results show that a precise payload positioning was achieved. AHL-ZVDD has superior performances in sway reduction and robustness.*

**KEYWORDS:** Crane System; Hoisting Length; Sway reduction; Zero Vibration Derivative Shaper

## 1.0 INTRODUCTION

Developments in large-scale manufacturing have seen the rise of crane systems deployed in industries. Other sectors of the economy such as transportation have also benefitted from the use of cranes. Because of the huge importance attached to crane use in industries, it has become necessary to have the cranes operating with high speed, and minimum sway (Masoud et al, 2001). High-speed operation of cranes results in unwanted motions such as swinging, bouncing and twisting. It also has serious safety concerns and could affect the rate of production due to unwanted downtime and inaccurate positioning of the payload (Singhose, 2009). Because of the aforementioned challenges, it has become necessary to apply techniques that could limit these unwanted sways in the crane system.

A lot of researchers have focused on the control of oscillations in crane systems. Ha & Kang (2013) Stated that this can be categorized into two; feedforward control and feedback control. It also inferred that feedforward techniques can be employed to cancel system oscillations while feedback control can be used to achieve precision in load positioning. It can also be used to reduce unwanted oscillations. Bartulovi & Zu (2014) showed that although a combination of the two control strategies could result in a more

---

\*Corresponding author e-mail: nuratahir85@gmail.com

efficient system, the feedforward control helps in reducing the complexity and cost of feedback control.

Several attempts have been made to design and implement control strategies that could minimize or eliminate these unwanted motions so that the safety and efficiency of the crane systems can be guaranteed. Numerous techniques ranging from classical control to modern control have been presented. Uchiyama et al (2013) proposed residual load sway suppression using open loop control. Similarly, Ahmad et al (2009) compared the performance of feedforward input shaping and low pass filtering (LPF) for anti-sway control, they discovered that input shaping was more robust compared to LPF for erroneous natural frequency. Mohamed et al (2015) used command shaping technique to reduce vibrations in a single link flexible manipulator. This technique results in the suppression of oscillatory response.

In addition, Maleki & Singhose (2010), Ahmad et al (2009) and Sorensen et al (2007) have shown that input shapers can be applied to crane systems to reduce oscillations. Vaughan et al (2008) and Schaper et al (2013) showed that, although the use of open loop controllers alone makes the crane systems vulnerable to external disturbances, a combination of feedforward and feedback control can result in an efficient control system. Terashima et al (2007) proposed control of rotary crane using the straight transfer transformation method (STT), for sway and position control of the system. Le et al (2013) presented a partial feedback linearization (PFL) and adaptive sliding mode control (SMC) for sway suppression of a rotary crane in a situation of inaccurate model or poor parameter representation. Though it is simple to design and implement, PFL is highly affected by parameter variations.

Bartolini et al (2002), Tuan & Lee (2013) and Tuan et al (2013) also presented sliding mode control for position and sway reductions of the crane system. But Tai & Andrew (2015) showed that SMC is not very popular due to the fact that it dissipates a lot of energy which leads to system burn-out. Furthermore, Nakazono et al (2008) presented three-layered neural networks with genetic algorithm for vibration control of the rotary crane. Ahmad et al (2010) carried out Performance investigation of sway control using LQR and PD-type fuzzy controller in the presence of a disturbance. Al-mousa & Pratt (2000) presented a combined fuzzy logic and a delayed feedback controller for oscillation reduction of the rotary crane.

## **2.0 CRANE DYNAMICS**

A crane system is a machine designed for the transportation of heavy and large amounts of a load from one position to another. It is mostly used in construction sites and large industries. As shown in figure.1, a laboratory scale 3D system consists of three parts namely; the Cart, the Rail, and the Payload, giving three directions of motion.

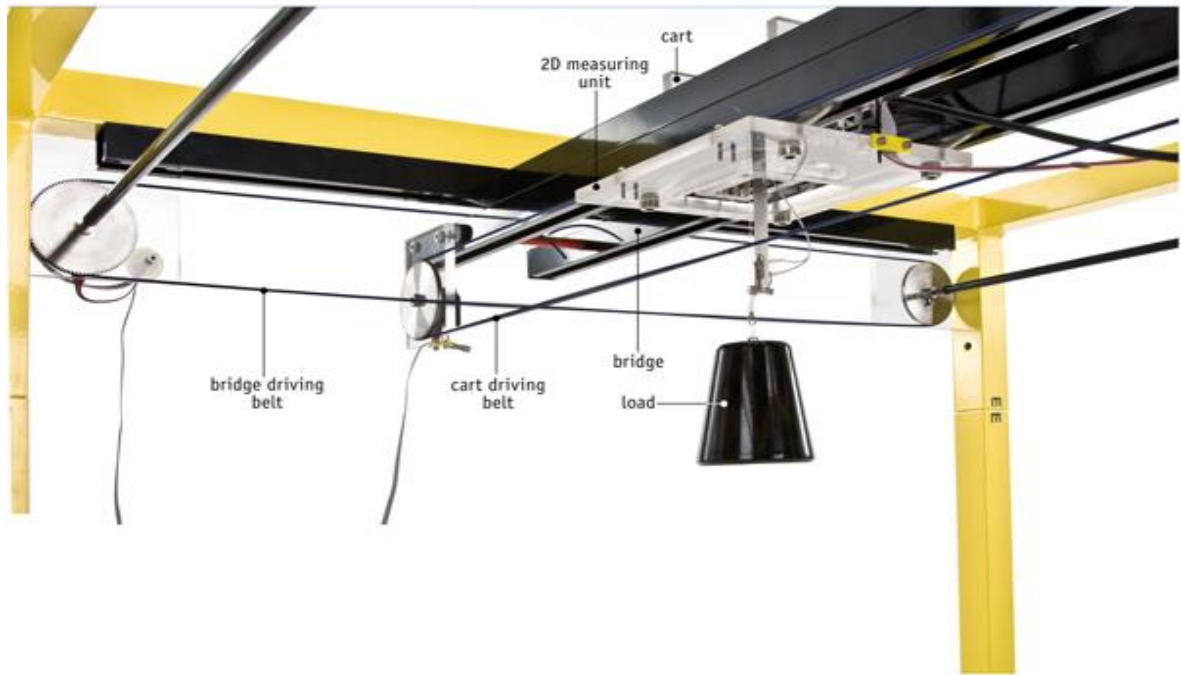


Figure 1. Laboratory Scale 3D Crane System

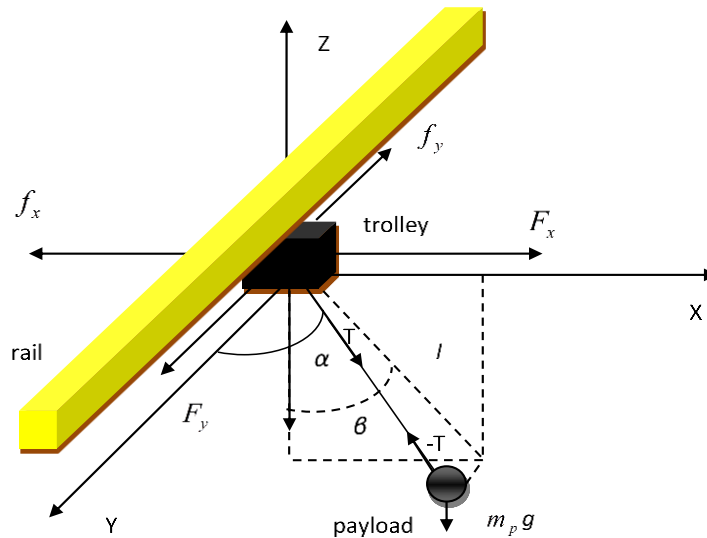


Figure 2. Schematic diagram and forces

That is, the cart moving along x-axis, the rail moving along y-axis and payload hoisting in z-axis. The schematic diagram of the 3D crane system is shown in figure 2. XYZ represents the coordinates; other system parameters are defined as; (Maghsoudi et al, 2014).

$\alpha$  angle of lift-line with Y-axis

$\beta$  angle between  $-Z$  and projection of the payload onto the XZ plane

$T$  reaction force in the payload cable acting on the cart

$F_x, F_y$  forces driving the rail and cart respectively

$F_z$  force lifting the payload

$f_x, f_y, f_z$  corresponding frictional forces

By definition,

$$\begin{aligned} \mu_1 &= \frac{m_p}{m_t}, \mu_2 = \frac{m_p}{m_t + m_r} \\ u_1 &= \frac{F_x}{m_t}, u_2 = \frac{F_y}{m_t + m_r}, u_3 = \frac{F_z}{m_p} \\ f_1 &= \frac{f_x}{m_t}, f_2 = \frac{f_y}{m_t + m_r}, f_3 = \frac{f_z}{m_p} \\ K_1 &= u_1 - f_1, K_2 = u_2 - f_2, K_3 = u_3 - f_3 \end{aligned}$$

Where;  $m_p, m_t$  and  $m_r$  are the payload mass, trolley mass (including gearbox, encoders, and DC motor) and moving rail respectively and  $l$  represents the length of the lift-line. The dynamic equations of motion of the crane can be obtained as given in (Maghsoudi et al, 2014).

$$\ddot{x}_p = K_2 + \mu_2 K_3 \sin \alpha \sin \beta \quad (1)$$

$$\ddot{y}_p = K_1 + \mu_1 K_3 \cos \alpha \quad (2)$$

$$\begin{aligned} \ddot{z}_p &= \ddot{z}_t + (\dot{x}_t^2 - l\dot{\alpha}^2 - l\dot{\beta}^2) \sin \alpha \sin \beta + 2l\dot{\alpha}\dot{\beta} \cos \alpha \cos \beta \\ &+ (2l\dot{\alpha}\dot{x}_t + l\dot{\alpha}\dot{y}_t) \cos \alpha \sin \beta + (2l\dot{\beta}\dot{y}_t + l\dot{\beta}\dot{x}_t) \sin \alpha \cos \beta \end{aligned} \quad (3)$$

$$\ddot{y}_p = \ddot{y}_t + (\dot{x}_t^2 - l\dot{\alpha}^2) \cos \alpha - (2l\dot{\alpha}\dot{x}_t + l\dot{\alpha}\dot{y}_t) \sin \alpha \quad (4)$$

$$\begin{aligned} \ddot{x}_p &= (-\dot{x}_t^2 + l\dot{\alpha}^2 + l\dot{\beta}^2) \sin \alpha \cos \beta + 2l\dot{\alpha}\dot{\beta} \cos \alpha \sin \beta \\ &- (2l\dot{\alpha}\dot{x}_t + l\dot{\alpha}\dot{y}_t) \cos \alpha \cos \beta + (2l\dot{\beta}\dot{y}_t + l\dot{\beta}\dot{x}_t) \sin \alpha \sin \beta \end{aligned} \quad (5)$$

Where,  $x_p, y_p$  and  $z_p$  are position of payload in X, Y and Z axes respectively.  $x_t$  and  $y_t$  are positions of trolley in X and Y axes. Dots represent derivative of the respective quantities.

Table 1 shows the parameters used for simulation and experiment which correspond to the crane system (Maghsoudi et al, 2014).

Table 1. System parameters

Variables	Values
Length of cable, $l$	0.72 m
Trolley mass, $m_t$	1.155 kg
Payload mass, $m_p$	1 kg
Mass of rail, $m_r$	2.2 kg
Frictional forces, $f_x, f_y, f_z$	100, 82, 75 Ns/m
Acceleration due to gravity, $g$	9.8 m/s

### 3.0 HYBRID CONTROLLER DESIGN

In this section, AHL-Shapers and MHL-Shapers were designed. Figure 3 shows the block diagram of the control schemes, where  $x$  is the trolley position and  $\theta$  is the sway angle. ZV, ZVD, and ZVDD are designed in each situation to suppress payload sways and PID was incorporated for trolley Position control. Comparative assessments are presented.

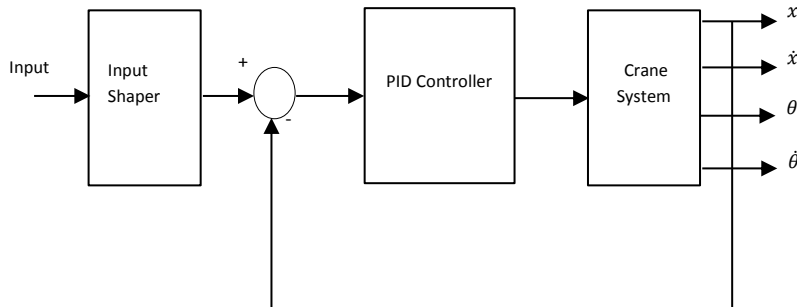


Figure 3. Block Diagram of Hybrid Control

### 3.1 Input Shaping

In this section, ZV, ZVD and ZVDD were designed. Using Curve fitting toolbox in the MATLAB software to determine the damping ratio and natural frequency of the system, with the input and output data obtained from the nonlinear crane system. The shapers were designed using different approaches that is, taking data at average load hoisting length and at maximum load hoisting length. Figure.4 shows an input shaping process while the parameters of this design are as recorded in Table 2 and Table 3.

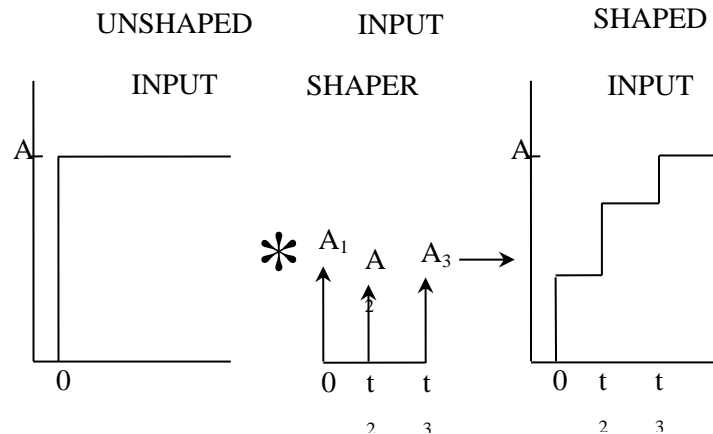


Figure 4. Input Shaping Process

The crane system was considered as 2<sup>nd</sup> order under-damped system as in (Ha & Kang, 2013).

$$G(s) = \frac{\omega^2}{s^2 + 2\zeta\omega s + \omega^2} \quad (6)$$

In which,  $\zeta$  and  $\omega$  is the damping ratio and natural frequency of the system respectively. The system response was expressed in time domain as ( Maleki & Singhose, 2010).

$$y(t) = \frac{A\omega}{\sqrt{(1-\zeta^2)}} e^{-\zeta\omega(t-t_0)} \sin\left(\omega(t-t_0)\sqrt{(1-\zeta^2)}\right) \quad (7)$$

Where  $t_0$  and  $A$  are the time instant and amplitude of the impulse. The response to an impulse sequence was obtained using superposition as;

$$y(t) = \sum_{i=1}^n \left[ \frac{A_i\omega_n}{\sqrt{(1-\zeta^2)}} e^{-\zeta\omega_n(t-t_i)} \right] \sin\left(\omega(t-t_i)\sqrt{(1-\zeta^2)}\right) \quad (8)$$

The residual vibration amplitude was obtained, with the following trigonometric.

$$\sum_{i=1}^n B_i \sin(\omega t + \beta_i) = A \sin(\omega t + \varphi) \quad (9)$$

In which;

$$A = \sqrt{\left(\sum_{i=1}^n B_i \cos(\beta_i)\right)^2 + \left(\sum_{i=1}^n B_i \sin(\beta_i)\right)^2} \quad (10)$$

Comparing the (8) and (9), we got

$$B_i = \frac{A_i\omega_n}{\sqrt{(1-\zeta^2)}} e^{-\zeta\omega_n(t-t_i)} \quad (11)$$

Rearranging (10) and (11) gives (Singhose, 2009).

$$A = \frac{\omega}{\sqrt{(1-\zeta^2)}} e^{-\zeta\omega t_n} \sqrt{R_1^2 + R_2^2} \quad (12)$$

Where;

$$R_1 = \sum_{i=1}^n A_i e^{\zeta\omega t_i} \sin\left(\omega t_i \sqrt{(1-\zeta^2)}\right)$$

$$R_2 = \sum_{i=1}^n A_i e^{\zeta\omega t_i} \cos\left(\omega t_i \sqrt{(1-\zeta^2)}\right)$$

At  $t=0$ , the residual oscillation amplitude from a unity magnitude was obtained as in (Blackburn et al, 2010).

$$A_{\uparrow} = \frac{\omega}{\sqrt{(1-\zeta^2)}} \quad (13)$$

In addition, the percentage residual vibration was obtained by, dividing (12) by (13) as;

$$R = \frac{A}{A_{\uparrow}} = e^{-\zeta\omega(t_n)} \sqrt{R_1^2 + R_2^2} \quad (14)$$

The zero vibration (ZV) constraint after the last impulse can be obtained by setting  $R_1$  and  $R_2$  of (14) to zero. The impulse amplitudes should be one hence the summation constraints are as (Ahmad et al, 2009).

$$\sum_{i=1}^n A_i = 1 \quad (15)$$

However, the first impulse time instant is set as,  $t_1 = 0$  Thus, the ZV parameters are obtained using its constraints by solving (14) and (15) as;

$$\begin{bmatrix} A_i \\ t_i \end{bmatrix} = \begin{bmatrix} \frac{1}{1+k} & \frac{k}{1+k} \\ 0 & \tau_d \end{bmatrix} \quad (16)$$

In which

$$\tau_d = \frac{\pi}{\omega \sqrt{(1-\zeta^2)}} \text{ and } k = e^{\frac{-\pi\zeta}{\sqrt{(1-\zeta^2)}}}$$

However, to increased robustness to frequency errors,  $R_1$ , and  $R_2$  derivatives are set to zero as;

$$\frac{\partial^i R_1}{\partial \omega^i} = 0 \text{ and } \frac{\partial^i R_2}{\partial \omega^i} = 0 \quad (17)$$

Hence, the constraints equations (14), (15) and (17) are solved to obtain the ZVD parameters as;

$$\begin{bmatrix} A_i \\ t_i \end{bmatrix} = \begin{bmatrix} \frac{1}{(1+k)^2} & \frac{2k}{(1+k)^2} & \frac{k^2}{(1+k)^2} \\ 0 & \tau_d & 2\tau_d \end{bmatrix} \quad (18)$$

Also, by using the second derivative of (17) and solving the constraints equations, the ZVD parameters were obtained as;

$$\begin{bmatrix} A_i \\ t_i \end{bmatrix} = \begin{bmatrix} \frac{1}{(1+k)^3} & \frac{3k}{(1+k)^3} & \frac{3k^2}{(1+k)^3} & \frac{k^3}{(1+k)^3} \\ 0 & \tau_d & 2\tau_d & 3\tau_d \end{bmatrix} \quad (19)$$

Equation (16), (18) and (19) were used to calculate the shapers parameters

Table 2. Shapers Parameters

	$l(m)$	$w_n$ (rad/s)	$\zeta$	$A_1$	$A_2$	$A_3$	$A_4$	$t_1$	$t_2$	$t_3$	$t_4$
MHL-ZV	0.72	3.73	0.006	0.5047	0.4953	0	0	0	0.8423	0	0
MHL-ZVD	0.72	3.73	0.006	0.2547	0.5192	0.2453	0	0	0.8423	1.6846	0
MHL-ZVDD	0.72	3.73	0.006	0.1286	0.3785	0.3714	0.125	0	0.8423	1.6846	2.5269

Table 3. Shapers Parameters

	$l(m)$	$w_n$ (rad/s)	$\zeta$	$A_1$	$A_2$	$A_3$	$A_4$	$t_1$	$t_2$	$t_3$	$t_4$
AHL-ZV	0.47	4.57	0.008	0.5063	0.4937	0	0	0	0.6874	0	0
AHL-ZVD	0.47	4.57	0.008	0.2563	0.4999	0.2438	0	0	0.6874	1.3748	0
AHL-ZVDD	0.47	4.57	0.008	0.1298	0.3769	0.3702	0.1204	0	0.6874	1.3748	2.0622

## 4.0 RESULTS AND DISCUSSIONS

In this section, the nonlinear crane system was simulated using step input to assess the AHL-Shapers and MHL-Shapers performance in vibrations suppression. PID incorporated with both AHL-Shapers and MHL-shapers are also assessed for setpoint tracking. A mean absolute error was employed as the performance index, is a very good measure of average error, level of sway reduction was measured and compared for various shapers. This is accomplished using the mean absolute errors of the shaped and unshaped responses. Also, the time response of the control algorithms was discussed and analyzed. The simulation results are presented and compared in this section.

### 4.1 Simulation result of nonlinear crane system with MHL-Shapers

The simulation results of nonlinear crane system with MHL-Shapers are as shown in Figure.5.MHL-ZV, MHL-ZVD, and MHL-ZVDD are presented and their results were compared. As shown in Table 4, MHL-ZVDD has shown a better performance in sways suppression, based on the percentage of sway reductions using mean absolute error.

### 4.2 Simulation result of nonlinear crane system with AHL-Shapers

The simulation results of nonlinear crane system with AHL-Shapers are as shown in Figure.6.AHL-ZV, AHL-ZVD, and AHL-ZVDD are also designed and presented, their performance is compared and assessed. It was observed that the performance of the shapers in sway reduction increased as the order of the derivatives increased as shown in Table 4.

### 4.3 Simulation result comparing AHL-Shapers with MHL-Shapers.

The performance of shapers from section 4.1 and 4.2 above were compared and evaluated. These were presented in Figure.7, 8 and 9. It was observed that AHL-Shapers shown a superior performance as compared with MHL-Shapers, this was as recorded in Table 4.

### 4.4 Simulation results using PID with the shapers incorporated

The nonlinear crane system was also simulated using PID with AHL-Shapers and PID with MHL-Shapers, for both set point tracking and vibrations control. Figure 10 and 11 show the performances of the hybrid algorithms, using the PID gains of  $K_p=2.21$ ,  $K_i=2.01$ , and  $K_d=0.53$ . From the two figures, it was observed that a good setpoint tracking was achieved. But increased in the derivative order of the shapers, increases delay in the system as shown in Table 5.

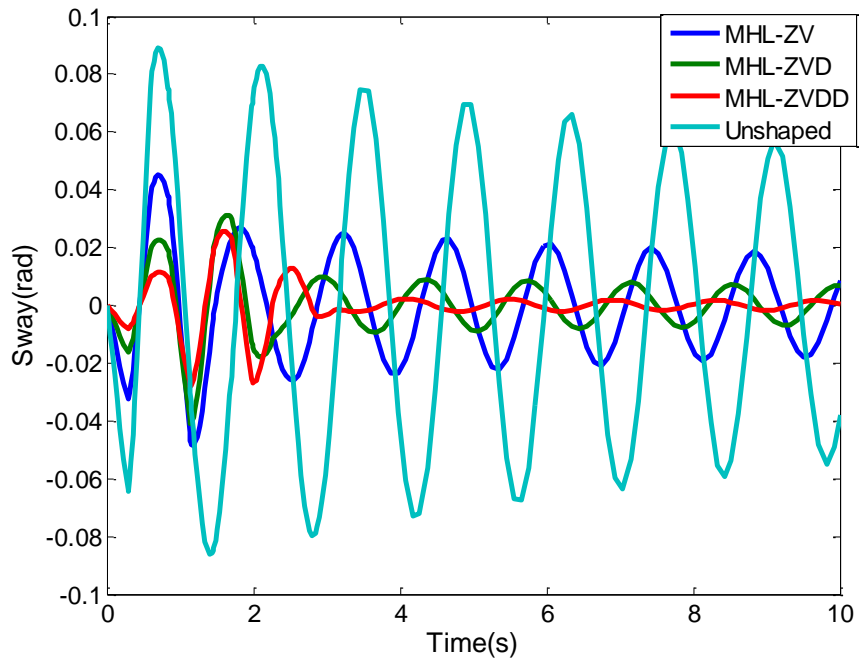


Figure 5. Trolley sways with maximum payload hoisting length

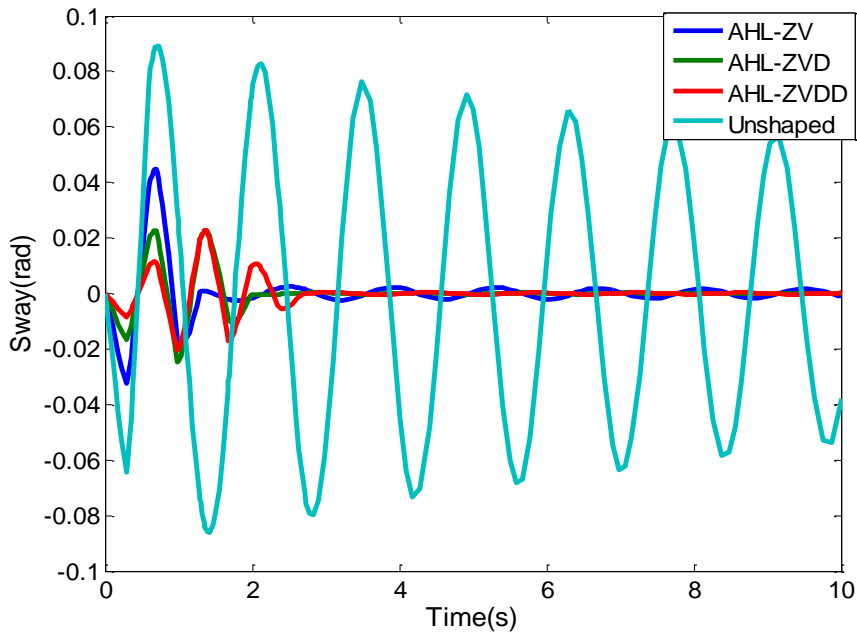


Figure 6. Trolley sways with average payload hoisting length

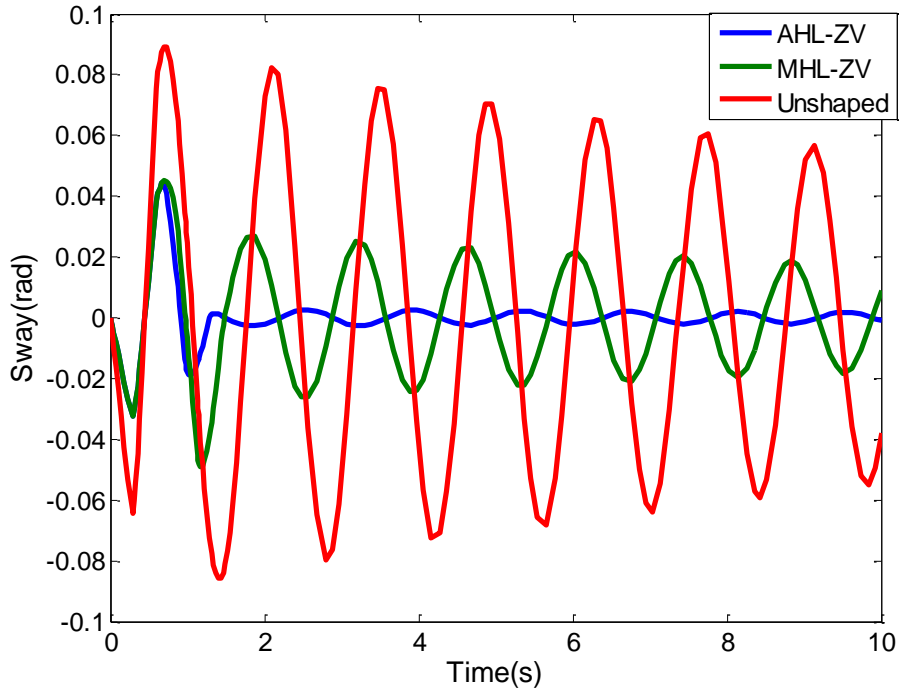


Figure 7. Trolley sways comparison using AHL-ZV and MHL-ZV

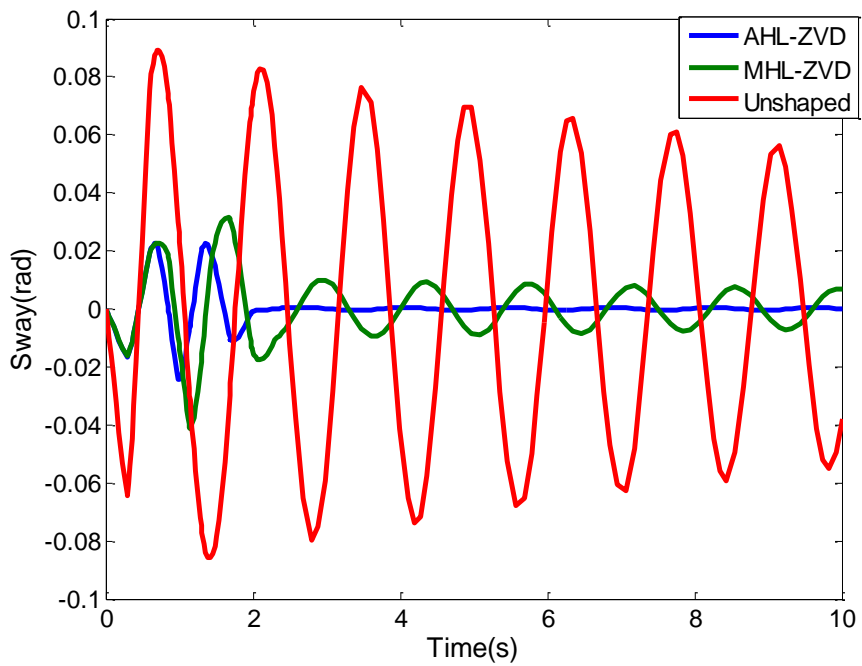


Figure 8. Trolley sways comparison using AHL-ZVD and MHL-ZVD

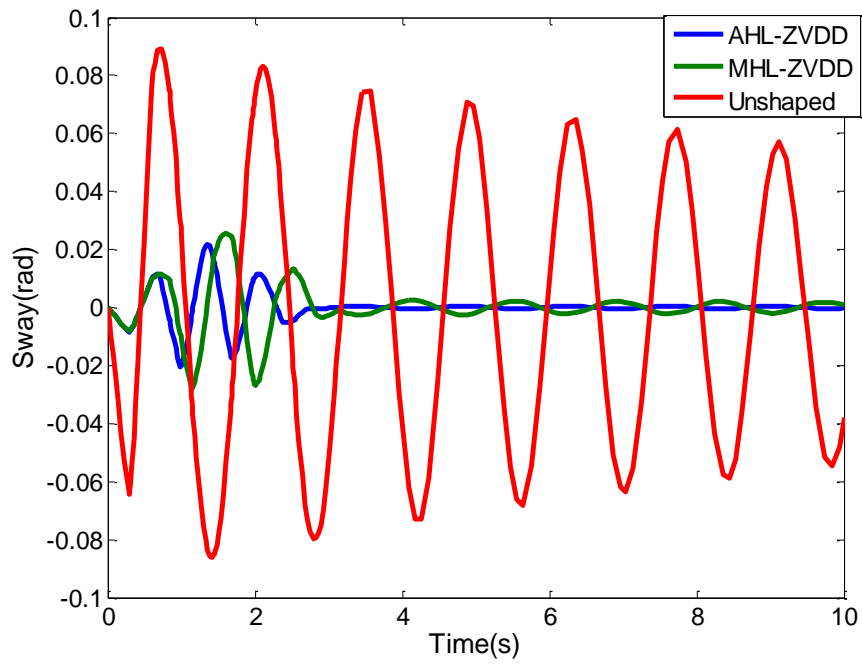


Figure 9. Trolley sway using comparison using AHL-ZVDD and MHL-ZVDD

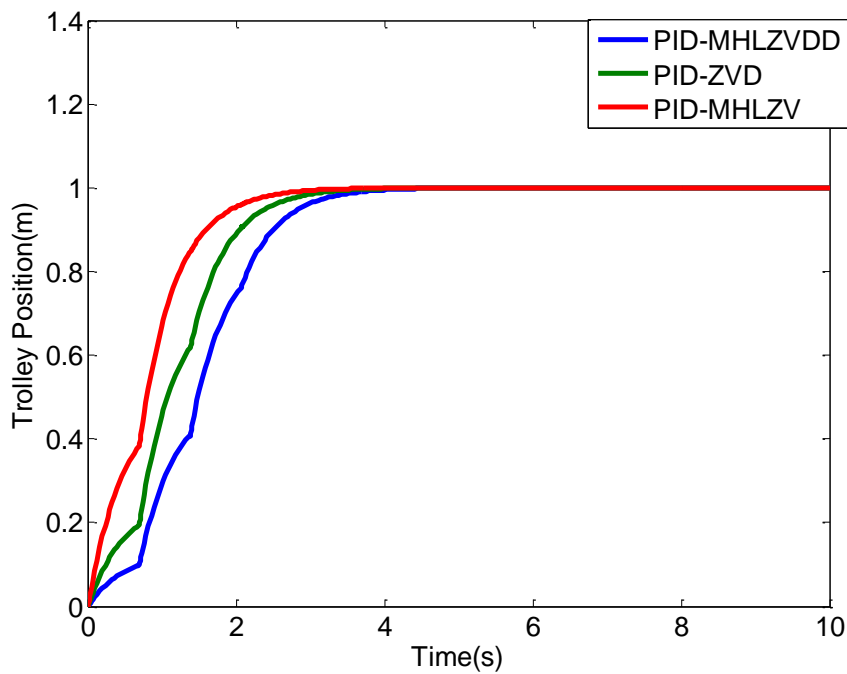


Figure 10. Trolley Position with Maximum Payload hoisting

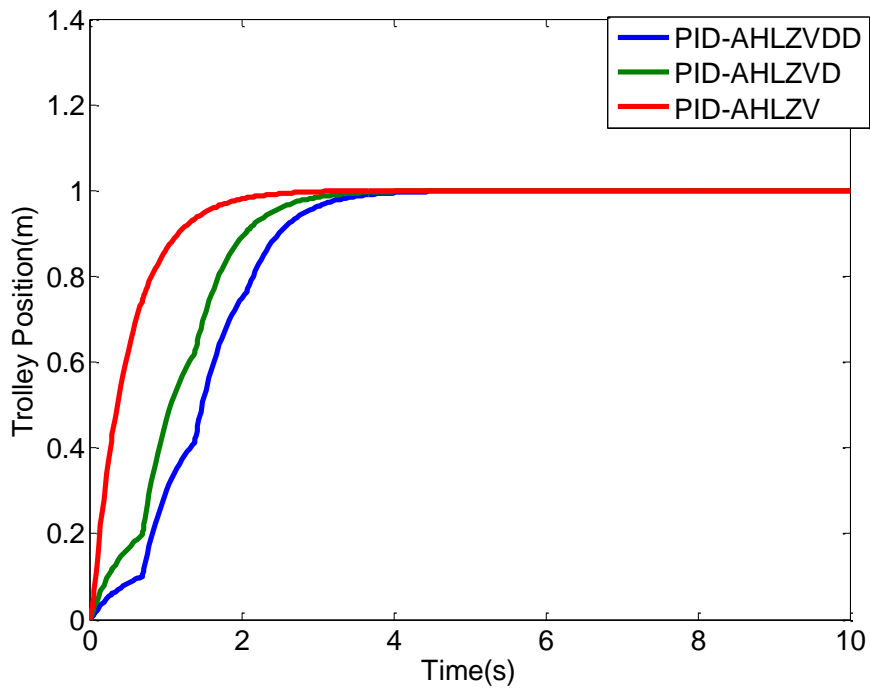


Figure 11. Trolley Position with Average Payload hoisting

Table 4. Level of sway reduction

Shaper	Percentage of sway reduction	
	AHL	MHL
ZV	84.2%	78.1%
ZVD	87.3%	83.4%
ZVDD	89.6%	86.2%

Table 5. Response time specifications

Shaper	Settling Time	
	AHL	MHL
ZV	1.85sec	2.20sec
ZVD	3.00sec	3.30sec
ZVDD	4.35sec	4.50sec

## **5.0 CONCLUSIONS**

This paper has presented hybrid control of nonlinear crane system. AHL-Shapers and MHL-Shapers, were designed to suppress vibrations while PID was incorporated for set point tracking control of the nonlinear crane system. The performances of the shapers are compared and MATLAB simulation results show that AHL-Shapers outperformed the MHL-Shapers in vibrations reduction. It was also observed that the higher the derivatives the better in vibrations suppression but the more the delay in the system. The control schemes have shown very good performances in payload positioning with load hoisting of crane system.

## **6.0 ACKNOWLEDGMENTS**

The authors gratefully acknowledged Ministry of Science, Technology, and Innovation (Project No. 03-01-06-SF1213) and UTM (Vote No. 4S103) for the financial support through Science Fund Research Grant.

## **7.0 REFERENCES**

- Masoud, Z.N., Nayfeh, A.H Abdel-Rahman E.M (2001). Dynamics and Control of Cranes : A Review. *Journal of Vibration and Control*, Vol.9 pp. 863–908,.
- Singhose, W, (2009). Command Shaping for Flexible Systems: A Review of the First 50 Years. *International journal of precision engineering and manufacturing*, 10(4), pp. 153-168
- Ha, M. and Kang, C., (2013). Experimental Analysis of Natural Frequency Error to Residual Vibration in ZV, ZVD, and ZVDD Shapers,"10<sup>th</sup> International Conference on Ubiquitous Robots and Ambient Intelligence Jeju South Korea, pp. 195–199.
- Bartulovi, M. and Zuzic, G., (2014). "Nonlinear Predictive Control of a Tower Crane using Reference Shaping Approach,"16<sup>th</sup> International Conference of Power Electronic and Motion Control, Antalya Turkey. no. 6, pp. 872–876,
- Al-mousa, A., (2015). Delayed Position-Feedback Controller for the Reduction of Payload Pendulations of Rotary Cranes," *J Vib. Control* Vol. 9, pp. 257–277.
- Uchiyama, N., Ouyang, H. and Sano, S. (2013). Simple rotary crane dynamics modeling and open-loop control for residual load sway suppression by only horizontal boom motion," *Mechatronics*, vol. 23, no. 8, pp. 1223–1236.
- Ahmad, M. A., Raja Ismail, R. M. T., Ramli, M. S., Zakaria, N. F., and Abd Ghani, N. M., (2009). Robust feed-forward schemes for anti-sway control of rotary crane," *CSSim 2009 - 1st Int. Conf. Comput. Intell. Model. Simul.*, pp. 17–22.

- Mohamed, Z., Chee, A. K., Hashim, A. W. I. M., Tokhi, M. O., Amin, S. H. M., Mamat, R., (2015). Techniques for vibration control of a flexible robot manipulator," *Robotica*, vol. 24, no. January 2006, pp. 499–511.
- Maleki E. and Singhose, W., (2010). Dynamics and Zero Vibration Input Shaping Control of a Small-Scale Boom Crane," 2010 American Control Conference, Baltimore, USA. pp. 2296–2301.
- Ahmad, M.A., Mohd, R., Raja, T. and Ramli, M. S. (2009). Input Shaping Techniques for Anti-sway Control of a 3-D Gantry Crane System, *Proc. IEEE Int. Conf. Mechatronics Autom. Chang. China*, pp. 2876–2881, August 2009.
- Sorensen, K. L., W. S. Å, and Dickerson, S. (2007). A controller enabling precise positioning and sway reduction in bridge and gantry cranes," *Control Eng. Pract.* 15 825–837, vol. 15, pp. 825–837.
- Vaughan, J., Yano, A., and Singhose, W. (2008). Performance comparison of robust negative input shapers, *Proc. Am. Control Conf.*, vol. 00, pp. 3257–3262.
- Schaper, U., Arnold, E., Sawodny, O., and Schneider K. (2013). Constrained real-time model-predictive reference trajectory planning for rotary cranes," *2013 IEEE/ASME Int. Conf. Adv. Intell. Mechatronics Hum. Wellbeing, AIM 2013*, pp. 680–685.
- Terashima, K., Shen, Y., and Yano K. (2007). Modeling and optimal control of a rotary crane using the straight transfer transformation method," *Control Eng. Pract.*, vol. 15, no. 9, pp. 1179–1192.
- Le, T. A., Dang, V., Ko, D. H., and An, T. N. (2013). Nonlinear controls of a rotating tower crane in conjunction with trolley motion," *Journal of System and Control Engineering*, vol. 227, no. 5, pp. 451–460.
- Bartolini, G., Pisano, A., and Usai, E. (2002). Second-order sliding-mode control of container cranes," *Automatica*, vol. 38, no. 10, pp. 1783–1790.
- Tuan L. A. and Lee, S. (2013). Sliding mode controls of double-pendulum crane systems†," *Journal of Mechanical Science and Technology*, vol. 27, no. 6, pp. 1863–1873.
- Tuan, L. A., Moon, S., Lee, W. G., and Lee, S. (2013). Adaptive sliding mode control of overhead cranes with varying cable length †," *Journal of Mechanical Science and Technology*, vol. 27, no. 3, pp. 885–893.
- Tai, C. and Andrew, K. (2015). Review of Control and Sensor System of Flexible Manipulator," *Journal of Intelligent and Robotic System*, Vol. 77 (1), pp. 187–213.
- Nakazono, K., Ohnishi, K., Kinjo, H., and Yamamoto, T. (2008). Vibration control of load for rotary crane system using neural network with GA-based training," *Artif. Life Robot.*, vol. 13, no. 1, pp. 98–101,

- Ahmad, M. A., Samin, R. E., and Zawawi, M. A. (2010). Comparison of Optimal and Intelligent Sway Control for a Lab-Scale Rotary Crane System," *2010 Second Int. Conf. Comput. Eng. Appl.*, pp. 229–234.
- Al-mousa, A. A., and Pratt, T. (2000). Control of Rotary Cranes Using Fuzzy Logic and Time-Delayed Position Feedback Control,"<http://hdl.handle.net/10919/36024>.
- Maghsoudi, M. J., Mohamed, Z., Husain, A. R., and Jaafar, H. I. (2014). Improved Input Shaping Technique for a Nonlinear System," 2014 IEEE International Conference on Control System, Computing and Engineering, 28 - 30 November 2014, Penang, Malaysia
- Blackburn, D., Singhose, W., Kitchen, J., Patrangenu, V., Lawrence, J., and Kamoi, T. (2010). Command Shaping for Nonlinear Crane Dynamics," *J. Vib. Control*.